The 6th International Supercritical CO_2 Power Cycles Symposium
March 27 - 29, 2018, Pittsburgh, Pennsylvania

The Ex-situ fatigue response of nickel superalloys in response to supercritical CO_2 exposure

Kyle Rozman
National Energy Technology Laboratory and
AECOM
Albany, OR USA
kyle.rozman@netl.doe.gov

Ömer N. Doğan
Materials Research Engineer
National Energy Technology Laboratory
Albany, OR USA
omer.dogan@netl.doe.gov

Gordon R. Holcomb
Materials Research Engineer
National Energy Technology Laboratory
Albany, OR USA
gordon.holcomb@netl.doe.gov

Jeffrey A. Hawk
Materials Research Engineer
National Energy Technology Laboratory
Albany, OR USA
jeffrey.hawk@netl.doe.gov

Casey S. Carney
National Energy Technology Laboratory and
AECOM
Albany, OR USA
casey.carney@netl.doe.gov

Kyle Rozman is currently an employee of AECOM as a contractor to the United States Department of Energy - National Energy Technology Laboratory in Albany, OR, where he has worked since 2017. Kyle received his Ph.D. from Oregon State University in Materials Science in 2014. Kyle's research interests include environmental effects on fatigue and fracture of metallic materials.

Gordon Holcomb is a Materials Research Engineer in the Structural Materials Team in the Research & Innovation Center at NETL. He received his Ph.D. from the Ohio State University in Metallurgical Engineering in 1988. Current projects cover corrosion issues in fossil energy systems. He is the U.S. Lead for the Corrosion in Supercritical Fluids task in the US-UK Collaboration on Fossil Energy Research and Development, Advanced Materials Technology Area.

Casey Carney received his B.S. in chemistry and engineering physics from Hope College. He received his Ph.D. in Chemical Engineering from the University of Colorado in 2005. He is currently an employee of AECOM as a contractor to the United States Department of Energy - National Energy Technology Laboratory in Albany, OR, where he has worked since 2008. His recent research topics have included: oxy-combustion flame analysis, thermal decomposition kinetics, and materials performance in extreme combustion and supercritical CO2 environments.

Ömer Doğan is a Materials Research Engineer in the Structural Materials Team in the Research & Innovation Center at NETL. He received his Ph.D. from Case Western Reserve University in Materials Science & Engineering in 1990. Current research focuses on the evaluation and development of heat, corrosion, and wear resistant materials for applications in harsh environments.

Jeffrey Hawk is a Materials Research Engineer in the Structural Materials Team, Materials Engineering and Manufacturing, in the Research & Innovation Center at NETL. He received his Ph.D. from the University of Virginia in Materials Science in 1986. Current projects cover mechanical behavior and microstructural evolution in fossil energy systems.

Abstract

Fatigue is known to cause unexpected failures which can be financially expensive. All parts of turbines undergo fatigue, from thermal cycling of the casing to immense creep-fatigue of rotors to mechanical fatigue of airfoils. In addition to quantifying the response of materials to high and low cycle fatigue, knowledge of fatigue crack growth rates is important as they enable engineers to calculate the minimum life of structural components. Fatigue failure is particularly crucial to be evaluated in CO_2 environments as efficient energy conversion demands a shift from traditional turbine working fluids of high pressure steam to CO_2. As a preliminary investigation, compact tension specimens of Haynes 282 and Inconel 625 were exposed to supercritical CO_2 at 730 ^oC at 200 bar for 500 hours. Additional specimens were also exposed to CO_2 at 730 ^oC and 1 bar for 500 hours and supercritical steam at 730^oC under 200 bar for 500 hours. The subsequent room temperature crack growth threshold was measured and reported. This paper will discuss the effect prior exposure had on fatigue thresholds. Crack growth rates and fracture surfaces were examined then compared between alloys and exposure conditions.

Introduction

With the transition from steam to supercritical CO_2 (sCO_2) as a turbine working fluid for power production, significant research efforts must be undertaken to compare the performance in sCO_2 to steam conditions. Past symposiums have featured many studies on temperature and corrosion of alloys suitable for A-USC and sCO_2 environments. However, only a few studies have explored relevant mechanical properties. Keiser et al. (Keiser et al. 2015) placed C-ring tests in a sCO_2 autoclave for 500 hours and found no signs of stress corrosion cracking on various steels and superalloys. Stresses were reported to 75, 85 and 95% of 500 hour rupture stress. While internal oxidation was found, the depth was limited to 7-10 μm, which is consistent with unstressed 500 hour exposures to similar nickel superalloys, see Holcomb et al. (Holcomb et al. 2015) which suggests only oxidation damage was detected. No discussion on bolt material and thread stress were found. Further discussion on the diameters of the C-rings before and after exposure would be useful to determine if the bolts relaxed during exposure. Keiser et al. only provided a presentation and not a manuscript where such details could be found. While the failure to detect signs of stress corrosion cracking may mean alloys are immune to stress corrosion cracking in sCO_2 conditions, it may also be that the bolt applying the

force crept and relaxed under the 500 hour exposure. A suggested experiment would be to place a control ring stressed to 110% of rupture stress. Should the control ring not rupture, then the bolt is likely relaxing.

Other studies tested the effect of a 500 hour exposure on tensile properties of various alloys (Pint et al. 2015). Pint et al., exposed 310H, EBright, 740 and 247 to CO_2 at various pressures at 750ºC for 500 hours and subsequently performed Ex-situ room temperature tensile tests on small specimens. For steels (310H and EBright), ultimate tensile strength (UTS) was unaffected while rupture ductility was increased for specimens exposed to 300 bar CO_2. For Ni-superalloy Inconel 740, UTS increased while rupture ductility decreased. Pint et al., suggested Inconel 740 "self-aged" under exposure conditions, which suggests the material was tested in a solution annealed state. The effect of 500 hours at 750ºC was most likely a single step aging process to grow gamma prime (γ'), a hardening phase in nickel superalloys, rather than some change due to CO_2 exposure.

One surprising result was that exposure (or "pre-oxidation") to both steam and argon reduced total creep lifetime and increased rupture ductility (Dryepondt et al. 2012). While this result is unanticipated, re-polished steam exposed specimens maintained a reduction in creep life and exacerbated rupture ductility, suggesting this phenomenon is not exclusively related to the oxidation damage.

Lacking from the literature are any studies on the effect of CO_2 on crack growth. Crack growth is an important design aspect in determining inspection intervals for critical structural parts. Engineers assume crack lengths exist just below detectable limits and use crack growth rates to assess minimum elapsed time for inspection. Crack growth rates, $\Delta a/\Delta N$, are typically plotted against the stress intensity range, ΔK, on a log-log scale. Crack growth rates represent crack extension per cycle, typically in *m/cycle*. The stress intensity range is a linear elastic mechanics factor normalizing the effects of crack length, applied stress and local geometry and is measured in $MPa\sqrt{m}$.

Crack growth rates are empirically observed to always follow a threshold, steady state and rapid fracture regime (Suresh 1998). Threshold crack growth occurs predominantly by single dislocation plane slip exiting at the crack tip (Forsyth 1962). In the threshold regime microstructural features such as precipitates, carbides and grain boundaries influence crack growth rates as dislocation glide may be impeded at these microstructural features. In the steady state regime, multiple dislocation slip systems contribute to crack tip extension. Therefore, crack growth is less sensitive to microstructural features. Steady state crack growth is observed to follow the Paris' law (Paris and Erdogan 1963), see Equation 1. The rapid fracture regime involves high ΔK and crack growth rates over mm/cycle; subsequently, it is of little practical engineering use. With the increased sensitivity of crack growth rates to microstructural features, threshold crack growth experiments were chosen for this research.

$$da/dN = C\Delta K^m$$

Equation 1. The Paris' Law, an empirical relationship between crack growth rate and stress intensity range

This research builds upon other Ex-situ sCO_2 research, testing the effect of sCO_2 exposure on fatigue crack growth thresholds in two classes of Ni-based superalloys; a precipitate hardened alloy, Haynes 282 and a solid solution strengthened alloy, Inconel 625. Thresholds are

compared to unexposed specimens, supercritical water (sH_2O) exposed specimens and 1 bar CO_2 gas (aCO_2) exposed specimens. Comparing exposed specimens to the unexposed specimens will show how severe any fatigue threshold shift is, while comparing to sH_2O and aCO_2, will show how the material behaves relative to typical steam turbine conditions and if there is any pressure effect of CO_2.

Materials and experimental procedure

Haynes 282 is a precipitate hardened superalloy with high strength at temperature due to the γ' precipitates. Due to its nickel and chrome content Haynes 282 has better corrosion resistance than typical stainless steels, however, it is not as good as solid solution strengthened nickel superalloys with higher chrome content. Inconel 625 is a solid solution strengthened superalloy with excellent corrosion resistance, however, it has lower mechanical strength relative to Haynes 282. Haynes 282 was received in plate form in the solution annealed state. The Haynes 282 plate was peak aged using the standard heat treat schedule of 1010°C for 2 hours followed by an air cool then aging at 788°C for 8 hours and an air cool. Inconel 625 was also received in solutionized plate form. No further heat treatments were done for Inconel 625.

Compact tension specimens with dimensions of 23 x 22 x 3.1 mm^3 were machined from each material. Three specimens were left unexposed, three were exposed to sCO_2 at 730°C at 207 bar for 500 hours, three were exposed to aCO_2 at 730°C at 1 bar for 500 hours and three were exposed to sH_2O at 730°C at 207 bar for 500 hours for a total of 12 specimens from each alloy. Further exposure details can be found in Holcomb et al. (Holcomb et al. 2015).

Crack growth threshold experiments were performed in accordance with ASTM E647 (ASTM E647). Precracking was performed at 25 Hz with a load ratio of 0.1. Precracking began with ΔK of18 MPa√m and finished at ΔK of ~15 MPa√m for Haynes 282 and ΔK of ~14 MPa√m for Inconel 625. The load shedding constant for precracking was -160 mm^{-1}. Precracking is important to generate a consistent sharp crack free of residual stress.

Testing frequency was selected at 40 Hz and load ratio was 0.1. Crack length, cycle count and load were recorded in increments of 0.01 mm of crack extension. Crack length was measured using back face compliance, which can be found in ASTM E647. Threshold values are reported in accordance with the linear intercept technique in ASTM E647.

One specimen of each exposure condition was selected for cross-sectional analysis. A corner was cut from the back face of the specimen, mounted and polished using standard metallography techniques. Specimens were etched using ASTM etchant #88 (ASTM E407). Imaging was done on a FEI inspect F electron microscope.

Hardness testing was done on a Brinell micro-hardness tester with an indent load of 200 g. The chosen indenter was of the Knoop type. Hardness results are presented as an average of seven indents with error bars representing one standard deviation of the data. Before indenting, all surfaces were polished to a 1200 grit finish.

Results

The corrosion results for Haynes 282 have been published (Holcomb et al. 2015, Holcomb et al. 2016). The alloy showed internal corrosion and recrystallization with depletion of chromium and γ'-forming elements at a depth up to 10 μm for CO_2 exposures, Figure 1a-b. Scale thickness was around 2 μm in all environments. Internal oxidation and recrystallization were less severe

for Haynes 282 in sH_2O compared to CO_2 environments, with corrosion depth limited to less than 5 µm, Figure 1c.

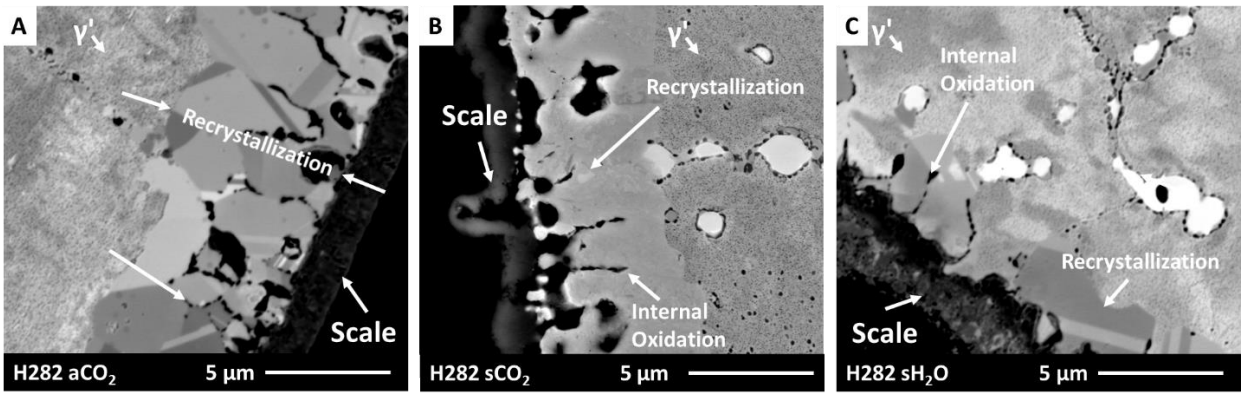

Figure 1. SEM micrographs of Haynes 282 after exposure of 500 hours in at 730°C in various environments. (A) Exposed to aCO_2 at 207 bar, (B) Exposed to sCO_2 at 207 bar, (C) Exposed to sH_2O at 207 bar.

For Inconel 625 a similar microstructural response was found as to Haynes 282. Detailed corrosion results for Inconel 625, including rates and elemental mapping can be found in Holcomb et al., 2016. Internal oxidation, recrystallization and oxide scales were present. Unlike Haynes 282, a detrimental phase, δ, was formed after the 500 hour exposures. Identified by its acicular morphology, δ can act to lower strength by consuming γ”-forming elements (Mathew et al., 2004). Scale thickness was <1 µm for all exposures, Figure 2a-c. Internal oxidation and recrystallization were limited to depths of 2-4 µm for all exposures, with the specimen exposed to sH_2O showing less magnitude of corrosion damage, Figure 2c.

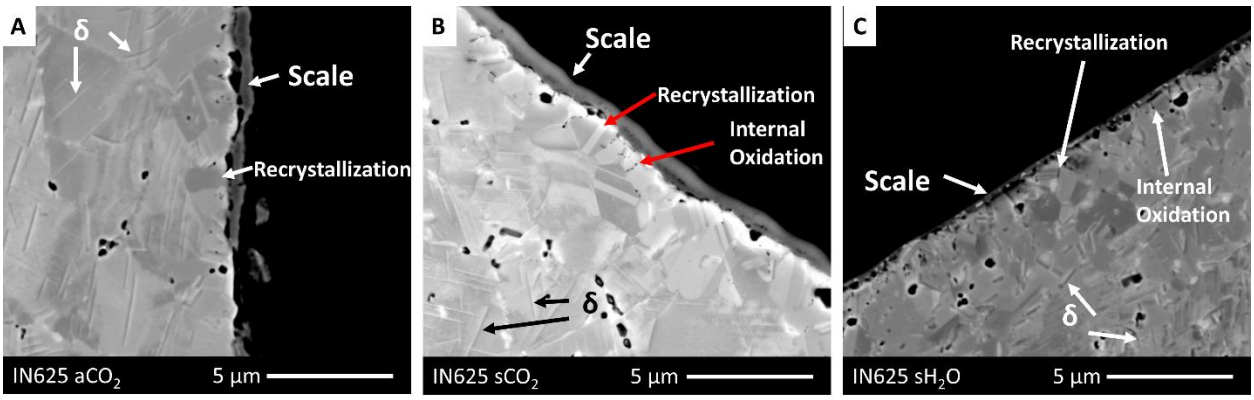

Figure 2. SEM micrographs of Inconel 625 after exposure of 500 hours in at 730°C in various environments. (A) Exposed to aCO_2 at 207 bar, (B) Exposed to sCO_2 at 207 bar, (C) Exposed to sH_2O at 207 bar.

The effect of exposure at 730°C for 500 hours on fatigue crack growth thresholds (ΔK_{th}) is shown in Figure 3a-b. Both alloys showed a slight reduction of ΔK_{th}. The measurement of ΔK_{th} for sH_2O was incomplete at this time. Repeat experiments are plotted for Haynes 282, while they have not been completed at this time for Inconel 625, except for the control specimen, which is plotted in green in Figure 3b. Regarding Figure 3b, the open green symbol shows

excellent experimental repeatability across laboratories, with solid symbols tested at the National Energy Technology Laboratory, and hollow symbols tested at Oregon State University.

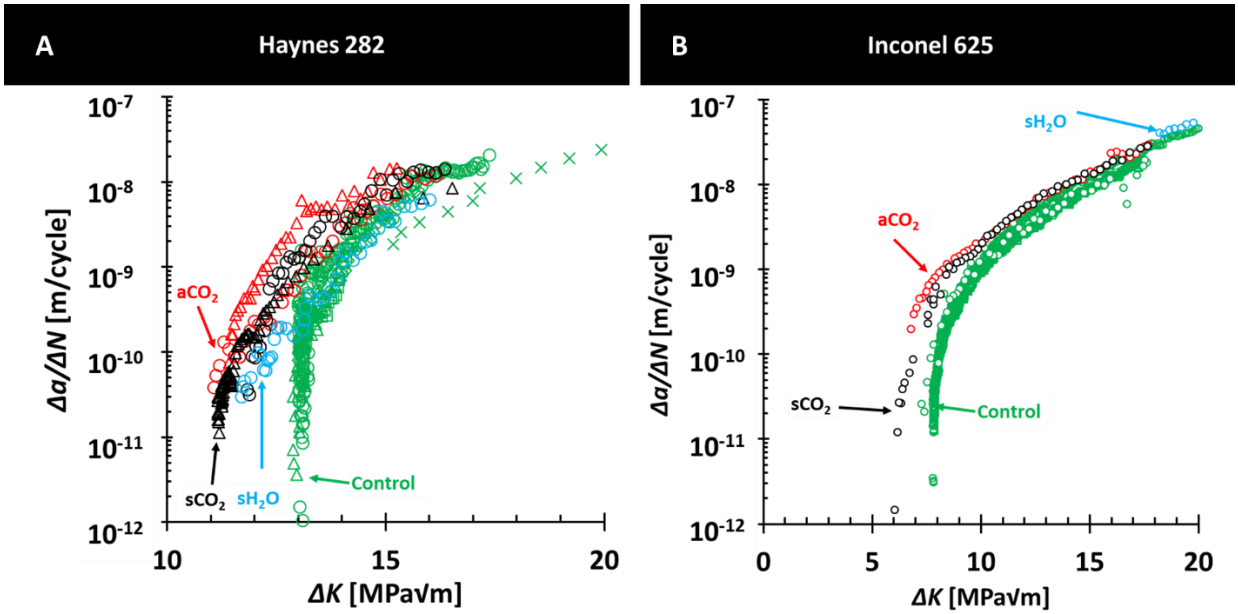

Figure 3. Fatigue crack growth thresholds after exposure to CO_2 and steam at 730°C for 500 hours at various pressures. (A) Haynes 282 and (B) Inconel 625.

Crack growth threshold was calculated as per ASTM E647 and tabulated in Table 1. For Haynes 282, ΔK_{th} was reduced by ~1.4 MPa√m from 13.1 MPa√m for control specimens in the as received state, to 11.6 MPa√m for specimens exposed to the various environments. For Inconel 625 this reduction in ΔK_{th} was reduced ~1.3 MPa√m from 7.9 MPa√m for the control specimens to ~6.6 for specimens exposed to CO_2 at 730°C for 500 hours at various pressures.

	ΔK_{th} [MPa√m]	
Average of:	H282	IN625
As received	13.1	7.9
aCO_2	11.3	6.3
sCO_2	11.6	7.0
sH_2O	11.9	-

Table 1. Crack growth thresholds at R=0.1 for Inconel 625 and Haynes 282. Thresholds are averaged except for Inconel 625 in CO_2 environments, where only one experiment was ran.

Discussion

A reduction in ΔK_{th} was shown for both alloys. This is rather surprising as corrosion damage is limited to a depth of 10 µm for both alloys. Microstructural changes due to heat exposure of 730°C for 500 hours are unanticipated as temperatures are below precipitate growth thresholds and not observed from Figures 1 and 2. The γ‘ precipitates in Haynes 282 do not show signs of excessive coarsening and studies up to 10,000 hours have shown that little coarsening takes place after γ‘ precipitates reach ~90 nm in diameter (Hawk et al. 2015). Hawk et al., found that for γ‘ to increase from 90 nm to 130 nm 8000 hours must elapse when aged at 760°C. With

experiments limited to 500 hours, γ‘ mean particle size is not expected to affect mechanical properties.

If the γ‘ unexpectedly overaged during the 500 hour exposure time, hardness measurements should show a drop in hardness for exposed specimens relative to the as received specimen. Micro-hardness measurements on Haynes 282 varied between 300 to 500 kg/mm^2. Measurements taken from the largest area of the specimen (Figure 4a location 1) were anomalously higher than specimen edges and cross-section (Figure 4a locations 2&3). However, hardness measurement variation overlapped indicating no measurable change in hardness from the environmental exposures. Transmission electron microscopy would be useful regarding this research to quantify microstructural changes of both Haynes 282 and Inconel 625. However, high magnification SEM images do not support γ’ growth or depletion in Haynes 282 in the bulk.

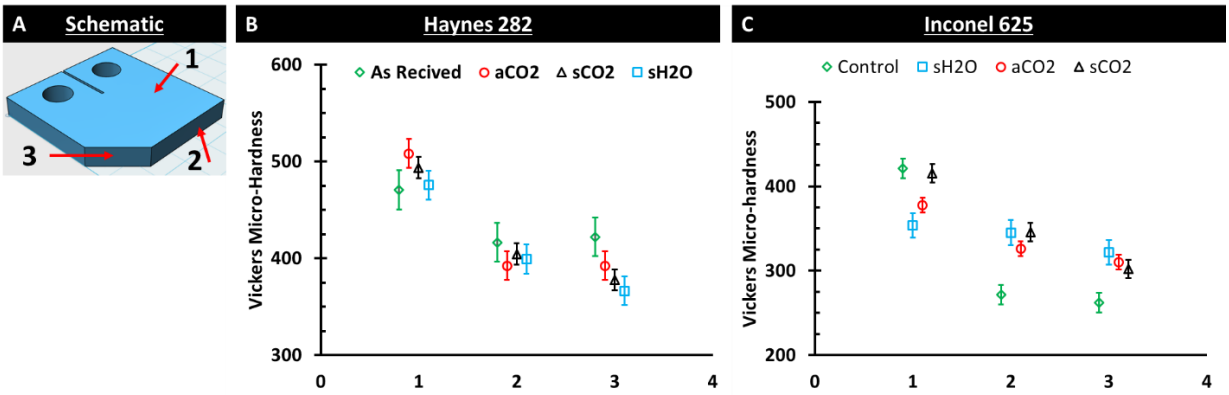

Figure 4. Hardness measurements of specimens after exposures to various environments at 730^{o}C for 500 hours. (A) Schematic showing hardness location, (B) Hardness measurements of Haynes 282, (C) Hardness measurements of Inconel 625.

For Inconel 625, δ like phases were optically detected in the microstructure. While δ precipitates are known to affect creep lifetimes adversely, they are unlikely to influence mechanical properties at high strain rates experienced by 40 Hz loading frequency. Peak hardness for Inconel 625 occurs at an ageing temperature of 700^{o}C (Cozar et al. 1991, Vernot-Loirer and Cortial 1991) which is only 30^{o}C below the exposure temperature of this work. Micro-hardness measurements were done to assess the effect of the δ precipitate, which varied between 300-415 kg/mm^2 for exposed specimens, while the as received specimen hardness was within or below those bounds at 270 kg/mm^2, Figure 4c. The increase in specimen hardness at locations 2&3 in Figure 4a is consistent with an aged material. A harder material would be expected to increase ΔK_{th} as dislocation glide is impeded from the δ phase. Because the ΔK_{th} was observed to decrease microstructural changes are unable to explain the change in ΔK_{th}.

Fracture surfaces were investigated near ΔK_{th} to determine if the corrosion layer had an influence on the fracture mechanism and if there was any change in fracture mode which may explain the reduction in ΔK_{th}. For Haynes 282 only stage one growth was observed, shown by tortuous crack path following dislocation slip planes, Figure 5a-d. With no evidence of change in fracture mode due to environmental exposures, the corrosion response is unlikely to explain the reduction in ΔK_{th}.

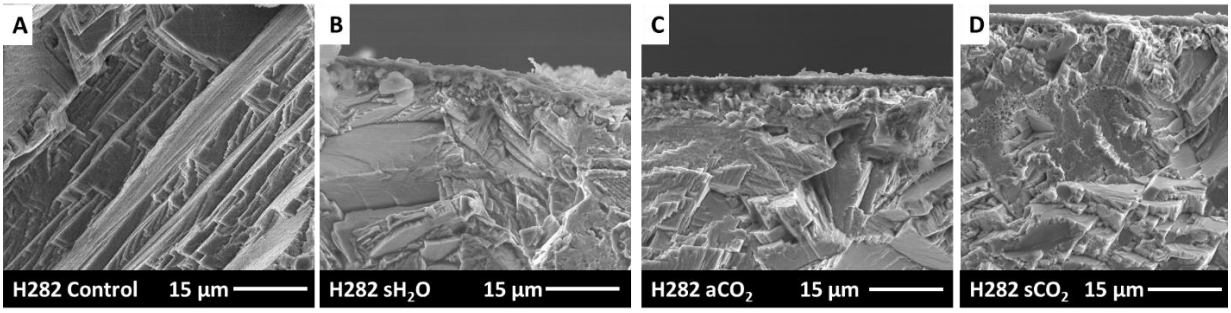

Figure 5. Fracture surface of Haynes 282 near crack growth threshold with crack growth direction left to right. (A) Control specimen, (B) Exposed to sH_2O at 730°C for 500 hours at 207 bar, (C) Exposed to aCO_2 at 730°C for 500 hours at 207 bar, (D) Exposed to sCO_2 at 730°C for 500 hours at 207 bar.

Additional evidence the crack growth behavior acted independently of the surface corrosion is supplied by overall crack front morphology. An idealized ductile crack path is shown in Figure 6b, where the crack front lags at surface edges. Should the surface corrosion interact with the crack front in such a way to accelerate the crack, the crack edges would be observed to lead the bulk crack front, Figure 6c. Comparing the real crack front, Figure 6a to Figure 6b&c shows typical ductile morphology. Therefore, it can be concluded that the effect of surface corrosion is not significant enough to alter crack growth from typical ductile mechanisms.

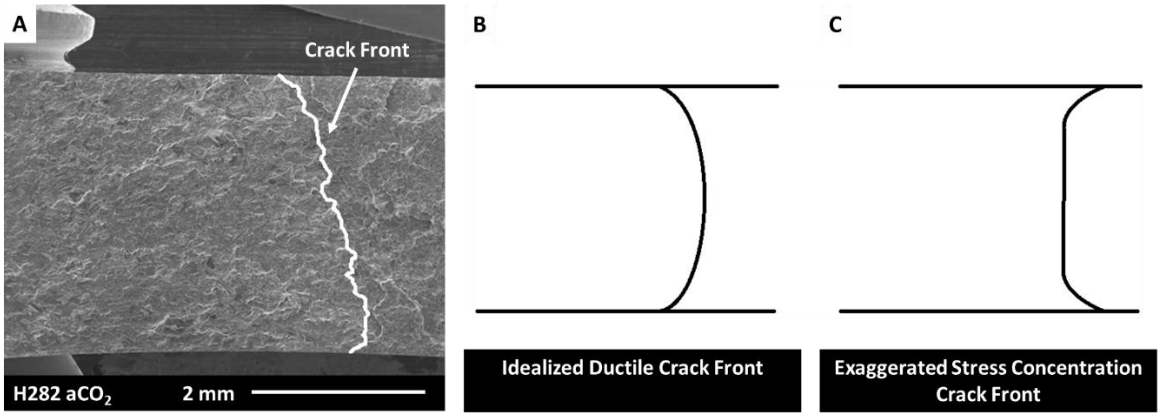

Figure 6. Showing crack front with crack growth direction from left to right. (A) Final crack front observed in Haynes 282 with exposure to aCO_2 gas (B) Schematic of ductile crack front (C) Exaggerated schematic where a stress concentration exists on specimen surface.

For Inconel 625, no change of fracture modes was observed, nor was the corrosion layer seen to influence fracture morphology, Figure 7a-c. Due to equipment failure, the sH_2O specimen for Inconel 625 was not tested. As with Haynes 282, there is no evidence of change in fracture morphology due to exposures. Hence, oxidation damages are unlikely to explain the reduction in ΔK_{th} for both alloys.

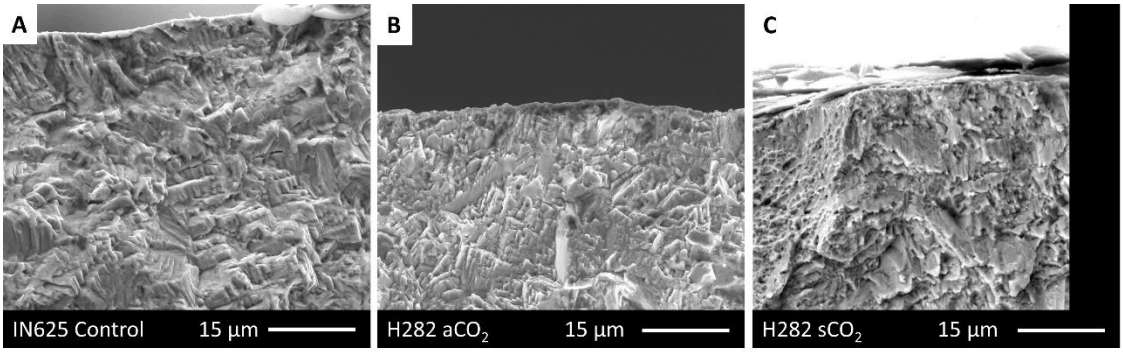

Figure 7. Fracture surface of Inconel 625 near crack growth threshold with crack growth direction right to left. (A) Control specimen, (B) Exposed to aCO_2 at 730°C for 500 hours at 207 bar, (C) Exposed to sCO_2 at 730°C for 500 hours at 207 bar.

The negligible influence of the corrosion layer is consistent with the previous research (Dryepondt et al. 2012) where a reduction in creep life was observed from exposure to steam and argon. Selected steam specimens were repolished after exposure, removing the oxidation layer and internal damage. Repolished specimens showed similar rupture times and minimum creep rates to that of unpolished creep specimens. Proving the reduction in creep life cannot be solely attributed to topical oxidation damage.

Further, it was shown that argon exposures suppressed γ' formation in alloy CCA617 (Dryepondt et al. 2012). Dryepondt et al. conjectured the partial pressure of oxygen may have influenced the γ' nucleation and growth. Dryepondt et al., also tested Inconel 740, a γ' former and Haynes 230, which is not a γ' former. A similar reduction in creep life was observed for Inconel 740, both after exposure and repolishing steam exposed specimens. However, for Haynes 230 creep rupture times and ductility overlapped for the as received specimens and steam exposed specimens. Because Haynes 230 is not a γ' former, the hypothesis that partial pressure of oxygen may influence the nucleation and growth of γ' precipitate may partially explain the phenomena. Unfortunately, Dryepondt et al. did not present measurements on γ' size or distribution. Further microstructural characterization comparing precipitate sizes and distribution is planned.

While there are arguments in the literature that microstructural changes may be occurring due to the partial pressure of oxygen influencing γ' formation, no additional evidence for this was found by the authors. An alternative hypothesis is that specimens had residual stresses and that the effect of time at temperature was to relieve residual stresses, hence the reduction in ΔK_{th}. The authors are preparing a separate manuscript to more fully address the residual stress. Preliminary results suggest that the decrease in ΔK_{th} was consistent with that measured by Bush et al. (Bush et al. 2000) where a change in manufacturing caused a decrease in ΔK_{th}. This reduction was attributed to a stress relief anneal. The location dependent hardness measurements in Figure 5 may alluded to retained residual stresses in C(T) specimens. Further testing is planned to elucidate the residual stresses in specimens. Threshold crack growth testing is planned on vacuum exposed specimens to isolate the effect of environmental exposure. Further residual stress is being quantified on the Haynes 282 plate material by a combination of hardness mapping of the plate and X-ray diffraction on specimens before and after vacuum exposure.

Conclusion

The effect of exposure to steam at 730°C at 207 bar for 500 hours and CO_2 at 730°C for 500 hours at both 207 bar and 1 bar on the crack growth threshold was measured. Results showed a reduction of about 1.5 MPa√m for both alloys. While microstructural changes were observed due to oxidation damage, depth was limited to around 10 μm and no evidence was found oxidation damages contributed to the macroscopic reduction in crack growth threshold. It is conjectured that precipitate changes may have lowered the crack growth threshold; however, quantification of the microstructure by TEM is needed. Equally possible is that crack growth specimens contained residual stresses which were annealed out during exposure. Further experiments are planned to quantify residual stresses and microstructural precipitates regarding their influence on crack growth thresholds.

Disclaimer

This project was funded by the Department of Energy, National Energy Technology Laboratory, an agency of the United States Government, through a support contract with AECOM. Neither the United States Government nor any agency thereof, nor any of their employees, nor AECOM, nor any of their employees, makes any warranty, expressed or implied, or assumes any legal liability or responsibility for the accuracy, completeness, or usefulness of any information, apparatus, product, or process disclosed, or represents that its use would not infringe privately owned rights. Reference herein to any specific commercial product, process, or service by trade name, trademark, manufacturer, or otherwise, does not necessarily constitute or imply its endorsement, recommendation, or favoring by the United States Government or any agency thereof. The views and opinions of authors expressed herein do not necessarily state or reflect those of the United States Government or any agency thereof.

Acknowledgements

This work was performed in support of the US Department of Energy's Fossil Energy Crosscutting Technology Research and Advanced Turbine Programs. The Research was executed through NETL Research and Innovation Center's Advanced Alloy Development Field Work Proposal. Research performed by AECOM Staff was conducted under the RES contract DE-FE0004000. The authors would like to acknowledge Oregon State University for use of experimental equipment and Drs. Jay Kruzic and Rawley Greene for fatigue crack growth software. The authors would also like to thank Dr. Mark Anderson at the University of Wisconsin—Madison for the work on sCO2 exposures.

References

ASTM E407-07, Standard Practice for Microetching Metals and Alloys, ASTM International, West Conshohocken, PA, 2015, www.astm.org DOI: 10.1520/E0407-07R15E01

ASTM E647—11 Standard Test Method for Measurement of Fatigue Crack Growth Rates, 2011, ASTM International, West Conshohocken, PA., www.astm.org DOI: 10.1520/E0647-15E01

Bush, R.W., Donald, J.K., Bucci, R.J. "Pitfalls to Avoid in Threshold Testing and its Interpretation," Fatigue Crack Growth Thresholds, Endurance Limits, and Design, ASTM STP 1372, 2000, J.C. Newman Jr., R.S. Piascik, eds., ASTM, West Conshohocken, PA, 269-284

Cozar, R., Rouby M., Mayonobe B. and Morizort C., page 423, in Ferrer, L., Pieraggi, B. and Uginet, J.F., Superalloys 718, 625 and Various Derivatives, Loria, E., (ed), the minerals metals and materials society 1991

Dryepondt, S., Unocic, K.A. and Pint, B.A., Materials and Corrosion, 63(10), 2012, 889-895 DOI: 10.1002/maco.201206694

Forsyth, P.J.E, A two stage process of fatigue crack growth. In Crack Propagation: Proceedings of Cranfield Symposium, 1962, 76-94, London: Her Majesty's Stationary Office.

Hawk, J.A., Cheng, T.-L., Sears, J.S., Jablonski, P.D., Wen, Y.-H., Journal of Materials Engineering and Performance, 24(11), 2015, 4171-4181 DOI: 10.1007/s11665-015-1711-y

Holcomb, G., Dogan, O., Carney, C., Rozman, K., Hawk, J., Anderson, M., Materials performance in supercritical co2 in comparison with atmospheric pressure co2 and supercritical steam, Paper #27, 5th International sCO2 power cycles symposium, 2016, San Antonio, Texas

Holcomb, G., Carney, C., Dogan, O., Corrosion Science, 109, 2016, 22-35 DOI: 10.1016/j.corsci.2016.03.018

Keiser, Leonard and McDowell, Characterization of turbomachinery materials for sCO2 application, Paper #203, 5th International sCO2 power cycles symposium, 2016, San Antonio, Texas

Mathew, M.D., Bhanu Sankara Rao, K., and Mannan S.L., Materials Science and Engineering A, 372, 2004, 327-333 DOI: 10.1016/j.msea.2004.01.042

Paris, P.C. and Erdogan, F. Journal of Basic Engineering, 84, 1963, 528-34

Pint, B., Brese, R., and Keiser, J., Effect of temperature and pressure on supercritical co2 compatibility of conventional structural alloys, Paper #56, 5th International sCO2 power cycles symposium, 2016, San Antonio, Texas

Suresh, S. *Fatigue of Materials*, 2nd ed. (Cambridge, UK: Cambridge University Press 1998) p. 341

Vernot-Loirer, C. and Cortial, F. page 423 in Ferrer, Pieraggi and Uginet, Superalloys 718, 625 and Various Derivatives, Loria, E., (ed), the minerals metals and materials society (1991)